SSCL-Preprint-56

SSCL-Preprint-56

Superconducting Super Collider Laboratory

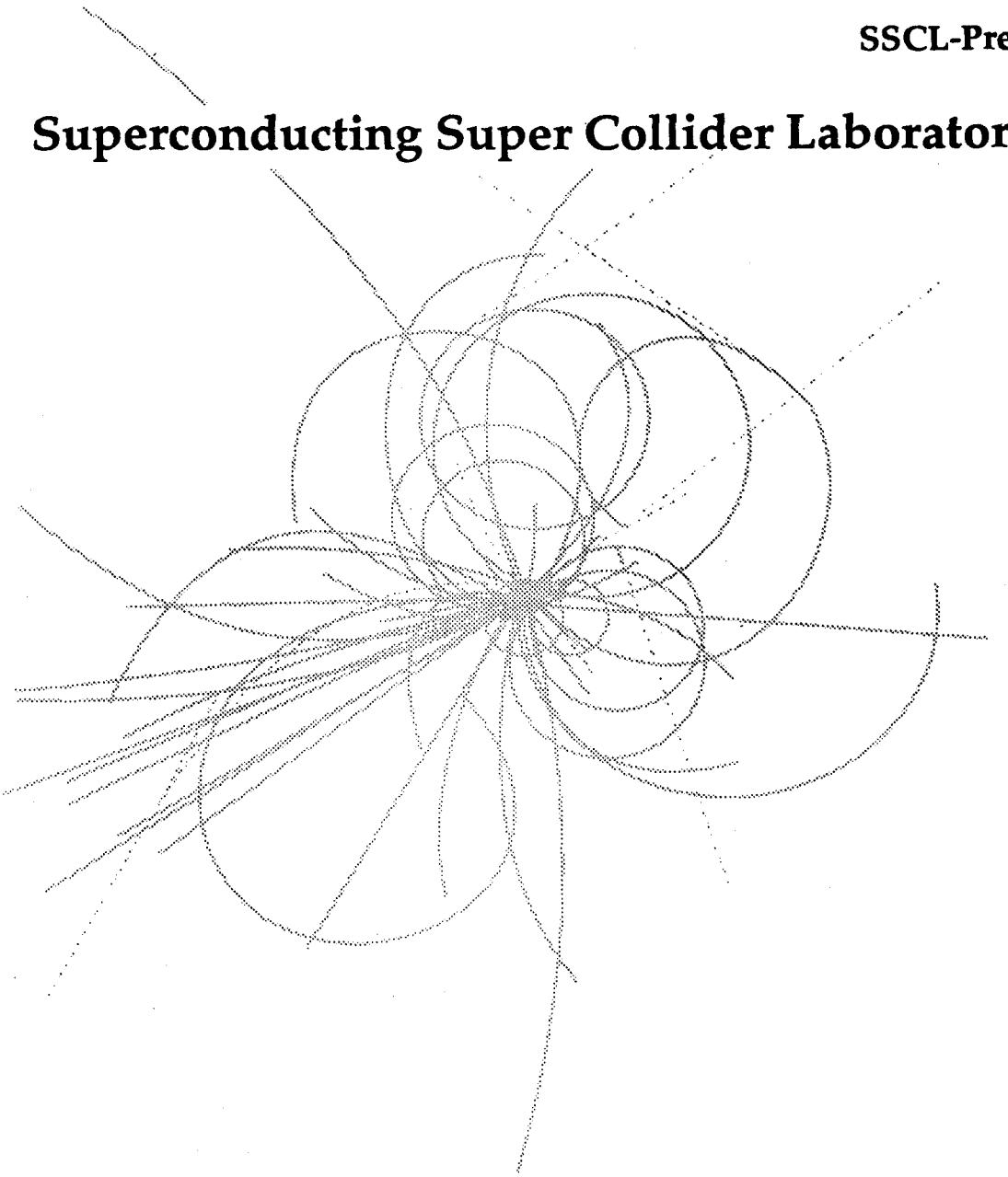

Transient Cooldown Stresses in Superconducting Collider Dipole Magnet

K. K. Leung and G. Snitchler

March 1992

To be published in *Supercollider 4*

SSCL-Preprint-56

Transient Cooldown Stresses in Superconducting Collider Dipole Magnet*

K. K. Leung and G. Snitchler

Superconducting Super Collider Laboratory†
2550 Beckleymeade Ave.
Dallas, TX 75237

March 1992

---

*Presented at the International Industrial Symposium on the Super Collider, New Orleans, March 4–6, 1992.

†Operated by the Universities Research Association, Inc., for the U.S. Department of Energy under Contract No. DE-AC35-89ER40486.

TRANSIENT COOLDOWN STRESSES IN SUPERCONDUCTING COLLIDER DIPOLE MAGNET

K. K. Leung and G. Snitchler

Magnet System Division
Superconducting Super Collider Laboratory*
2550 Beckleymeade Avenue
Dallas, TX 75237

ABSTRACT

The three-dimensional thermal transient stress in a collider dipole magnet (CDM) is evaluated and examined. The cooldown rate is one of the factors that determines the availability of the Superconducting Super Collider ring, but it is limited by stress in the magnet during cooldown. The main concerns are the effects of coil stress on stable operation and of shell stress on survival in long-term operation. Cost-effective operation can be attained if fastest cooldown-induced magnet stress would not exceed the safe operating stress of the magnet.

A 50-mm dipole magnet is modeled in the vertical split yoke configuration. Magnet components include shell, yoke, end yoke, collar, coil, and kapton insulation. These components are integrated by 3-D interface elements with preload but without friction. The cooldown condition is established by 4 K helium at 96 grams per second (gps) flowing in four bypass tubes and 4 gps to the beam tube annular area. The cooldown time is about 2 hours in most of the center section of the magnet and about 4 hours for the end sections, assuming that the end plate and the end yoke are also cooled down by the bypass flow.** Purposes of this study are to understand the stress-time history and maximum stress generated by the possible fastest cooldown condition and to demonstrate that non-linear thermal transient stress analysis can be performed in a workstation with limited computing resources. The results can be utilized to evaluate (1) the stress of the shell in long-term operation, (2) the fastest safe cooldown rate in the CDM, and (3) the cooldown time for the specified cooldown rate.

---

*Operated by the Universities Research Association, Inc., for the U.S. Department of Energy under Contract No. DE-AC35-89ER40486.

**Cooldown at the end is by mix-flow, and the G10 end assembly is not included in this simplified model.

INTRODUCTION

Three-dimension CDM thermal steady-state stress has been studied, and high stress is found in the shell.[1, 3] Two-dimension CDM thermal stress has also been studied, and the results are reported in Reference 2. ANSYS* is used to study the 3-D thermal transient effect on the CDM in the present analysis. The difference between a 2-D model and a 3-D model in thermal transient stress calculation is evaluated. Five models are used for this study. The models (A) and (B) are short models (5 cm), assembled with coil, collar, yoke, kapton, and shell. Each component is integrated with interface elements, which in thermal analysis represent the thermal contact resistance that can be experimentally confirmed. A 100% thermal contact area is assumed for all interfaces. This assumption is based upon the SSC magnet design that uses a line-to-line fit for all interfaces. The helium flow paths are represented by mass transport elements with specified flow velocities and heat transfer coefficient. Stress analysis is performed by converting the thermal elements into structural gap elements. The difference between models (A) and (B) is that the shell material property is linear elastic for model (A) and bilinear kinematic hardening for model (B). Models (C) and (D) are 30 cm long with components identical to models (A) and (B), with an end yoke and end plate added to the shell. Models (C) and (D) are used to study the cooldown stress on the shell in the area with differential rigidity of the end yoke to the body yoke and to study the joint stress at the end plate and shell. Model (E) is 15 m long and is used to study the temperature-time history of the CDM in the axial direction. This model is used for approximating the thermal boundary condition at the beam tube area because of the short model assumption for the present analysis.

CDM MODEL AND BOUNDARY CONDITIONS

The detail cold mass model is composed of several units. The units for the short model are:

(1) Steel Shell. A cylindrical shell made of 304 LN stainless steel with wall thickness of 0.5 cm. The shell is used as (a) a pressure boundary, (b) a thermal boundary, (c) a preloading device for the CDM components in limiting micro-movement under Lorentz force, and (d) an integrated element for CDM components in resisting external loads. The functions of (a) and (b) are employed in the present model. The functions of (c) and (d) are not used for this analysis and are expected to add stress to the CDM.

(2) Iron Yoke. Steel plates are laminated to form the yoke. The axial elastic modulus of the yoke is small in comparison to the solid steel and was assumed to be 5% of the modulus of the solid steel. Models (C) and (D) are used for modeling the end portions of the CDM in which the end yoke is added to support the end shell to reduce shell-bending stress, and the end plate is used to apply axial preload to the coil assembly.

(3) Collar. The collar is used for preloading the coils. The collared coils are the basic assembly of the cold mass in controlling the mechanical quench performance. Ovalization of the collared coil assembly is induced as the coils' internal stress acts on the collar. The position of coil assembly ovalization is approximated by the following technique: The horizontal boundary of the collared coil assembly is applied with vertical pressure determined by test. The deformation of the coils under such a loading condition is applied to the CDM model. The yoke, collar, and shell at the horizontal boundary have zero vertical deflection. The coils, collar, shell, and gap elements that connect to the vertical split yoke have zero deflection.

---

*ANSYS is a general-purpose, finite-element code developed by Swanson Analysis Systems, Inc.

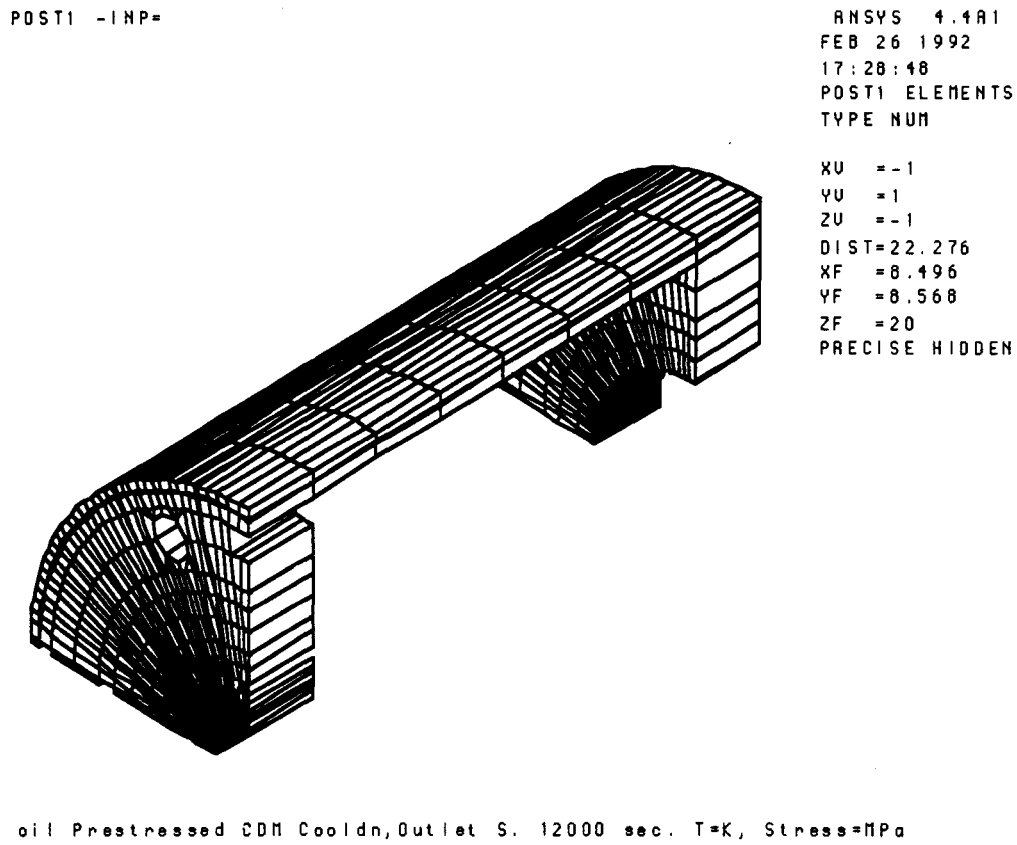

Figure 1. Detail Cold Mass Model at End Section.

(4) Coil Assembly. Both the inner coil and outer coil are modeled with wedges considered as part of the coils.

(5) Kapton Insulation. The Kapton is modeled in two different kinds of elements. In thermal analysis, radial-direction, solid-conduction paths are significant, and conduction bar elements are used for Kapton. The conduction bar elements are replaced by gap elements in order to evaluate the thermal stress on the magnet. The application of conduction bar elements is approximate because lateral heat transfer in the interface is not considered. But thermal contact resistance in tests indicates insignificant lateral heat flow because the peak and valley in the contact area break the lateral conduction paths.

(6) End Model. Models (C) and (D) are those with end yoke and end plate added to models (A) and (B). The cold mass shell is extended and overlapped to the end yoke without friction. The shell is modeled as an integrated part of the 3.8-cm-thick end plate. Conduction bars are used for heat flow to sink heat from the end yoke to the shell and to the bypass coolant. The end shell and the end plate have differential thermal capacitance, which would generate large thermal stress at the interface. The last model, model (E), is a 15-m-long CDM model. This model is a simplified 3-D model used to evaluate the thermal boundary condition of the CDM

The thermal boundary conditions are adiabatic at the $x = 0$ and $y = 0$ planes. These boundary conditions are transformed into more complex structural boundary conditions. In the thermal stress analysis, the boundaries are divided into many groups in order to match the vertical split yoke condition and the coils pre-deflected at the horizontal boundary. At $z = 0$, the axial boundary condition of the magnet is considered as follows: At the center of the 15-m CDM, a fixed translation boundary is observed because there is no thermal

movement in this center plane; the other end is subjected to axial compression load but the relaxation of the coils and other components reduces the axial compression load to an insignificant value at operation condition. The axial structural boundary condition of the model for the CDM is a fixed-free boundary condition.

LOADING CONDITIONS

Both thermal and mechanical loads are used in the dipole magnet model. The Lorentz force generated by the coil is not included in this model because the magnets are preloading to the point that the Lorentz force would not exceed the preload on the magnet components, as indicated in Reference 2. And there is no Lorentz force developed in the cooldown condition. The cooling condition at the magnet end assembly—including complex coolant flow to the G10 end coil assembly, the end plate, vessel head, and end yoke—are to be included in future study.

MODELING OBJECTIVES AND MODELING TECHNIQUE

Five different models are developed for the CDM with different objectives. Ideally these models can be combined into one with substantially greater computing resources. A workstation (Sparcstation 2) can perform non-linear, finite-element analysis by dividing the dipole model into many portions, with each portion as an independent model constructed for calculating a particular objective of the thermal transient stress problem. This method of modeling requires a trial procedure in order to maintain the model wave front that can be handled by the present workstation as well as by the network system. The Sun workstation is best for handling medium-sized thermal/structural analysis and is good for front-end applications such as mesh generation and geometry verification for more complex problems. The CDM thermal transient stress problem needs many load steps to evaluate the thermal stresses. The non-linear element and non-linear materials are first considered in the present analysis. The non-linear gap element and temperature-dependent material property are the basic requirements for the CDM thermal transient analysis. Elastro-plastic material properties in multi-linear form are needed to adequately address the relaxation of stress in components. The Sparcstation 2 can be used to select the most critical non-linear material properties for the particular component for large deformation effect at a particular time of the model. Both models (B) and (D) are employed to evaluate stress at the radial and azimuthal coil stresses and at the interfaces of the shell/end plate and shell/end yoke to determine the long-term operation cycles of the CDM. Using multi-linear kinematic or isotropic hardening behaviors for material properties can produce the best result in stress analysis. Limited by wave front of the Sun workstation, the classical bilinear kinematic hardening is applied in the present analysis. This simple material behavior does account for the Bauchinger effect by assuming that the yield surface translates only in the direction of yielding and does not grow in size. Model (E) is a simplified version of model (A), with axial length expanding to 15 m, but the wave front is minimized by using only significant elements in this particular analysis.

Transient temperature gradients are directly related to the CDM thermal stresses. Fast cooldown with liquid helium may create local thermal stress in the CDM because of different thermal capacitance of the yoke, end plate, end yoke, collar, coils, and shell. Under normal circumstances the thermal stress is greater than that obtained under steady-state condition because the transient gradients are always steeper. The surface thermal stresses in the shell can be expressed as $1.98\ (\Delta T * \Delta\alpha)\ E$.[6] The stress depends on the differential temperature and the coefficient of expansion between the yoke and shell wall and the elastic modulus E only.

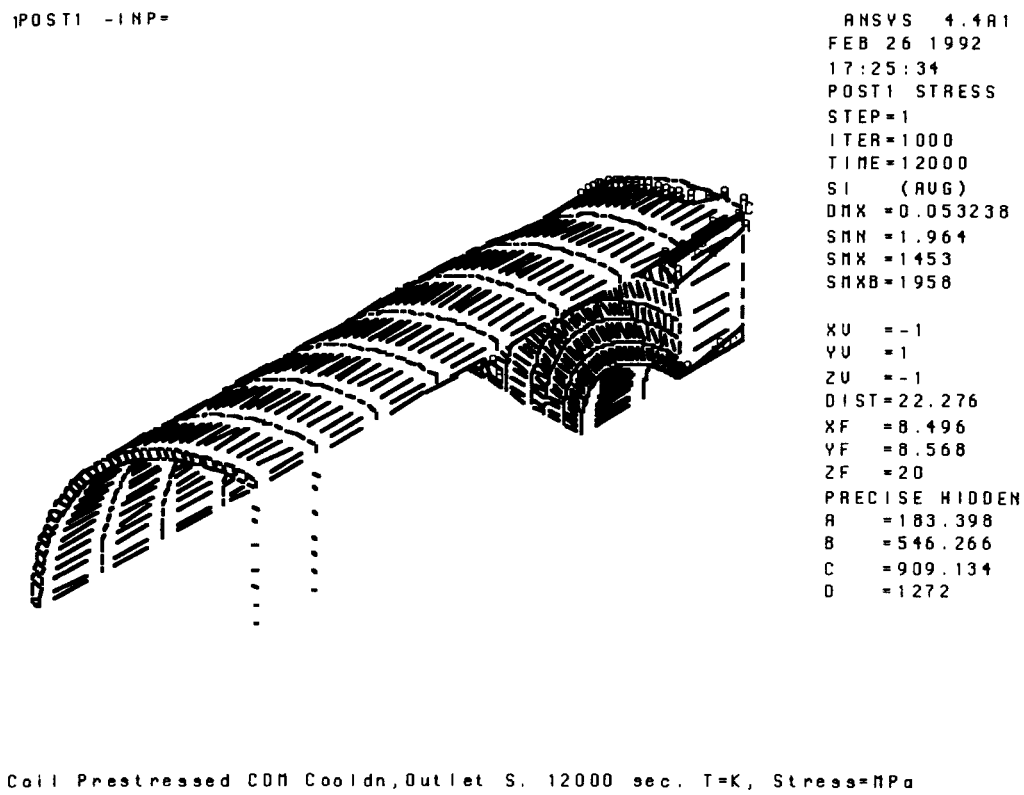

Figure 2. Thermal Transient Stress at Shell/End Plate Interfaces at 12,000 Seconds.

DISCUSSIONS

The calculated temperature and stress of model A are compared to the 2-D model results from Reference 2. The temperature-time history in the 2-D model is considered as a good approximation of the 3-D model. However, heat flow paths for the 3-D model are different from the 2-D model because of cavity and bypass tubes in the yoke. Particular heat paths in the 3-D model can be fitted to the 2-D model, and the CDM temperature-time history can be studied by using a 2-D model. The comparison of thermal transient stresses between the 2-D and 3-D models are difficult because local thermal transient gradients are not available in the 2-D model. Stresses are also sensitive to the three-dimensional geometry discontinuity and the boundary, which the 3-D model can describe in detail for investigation. Stress in the third dimension produces significant effects on the combined stress in components.[5, 6] The experimental azimuthal coil stress of the CDM is based upon a special strain gauge assembly design that uses a steel block attached to a strain gauge to register the coil/collar interface stress. The recorded strains on this block represent the average stress sensed by the block and provide no information on the peak stress in the coil. The fact that the finite-element result indicates higher stress than the test may be attributed to the averaging of stress by the strain gauge block in test.

The following observation has been made for the CDM model with 100 gps helium at 4 K as coolant. The time to steady-state condition at 4 K from room temperature is about 6000 seconds for the center section. For the end section in the present analysis, by assuming a cooling condition for simplicity and conservatism, the time to steady state is 14,000

seconds. The cooling time would be less in mix-flow cooling condition, and different thermal stress would be induced in the end plate, end shell, and vessel head area. This cooling condition would be better studied at a workstation with greater computing resources. The collared coils' maximum azimuthal stress is 155 MPa (23 ksi) at 12,000 seconds. The coil stress would be less if hyperelastic property of Kapton insulation is included in the present analysis. The shell/end plate interface combined stress is 1272 MPa (184 ksi), which is less than the tensile strength of 316 LN at 77 K (1517 Mpa) and 1697 Mpa at 4 K.[7] The present model does not associate the gap to the thermal contact resistance. The radiation between closely-spaced parallel surfaces with a diffuse reflectivity problem is not addressed in the present analysis. The difference in 2-D and 3-D thermal stress models is that the 3-D model produces critical information for the CDM design specifically in the area of high stress. The 2-D model is useful in providing information for the temperature-time history of the magnet in general. The coil stress is related to the shell stress and material non-linearities of the Kapton. A complete stress-time history of the coil and shell with consideration of multi-linear properties for all components under transient cooldown condition should be performed in the future, perhaps with a more powerful workstation.

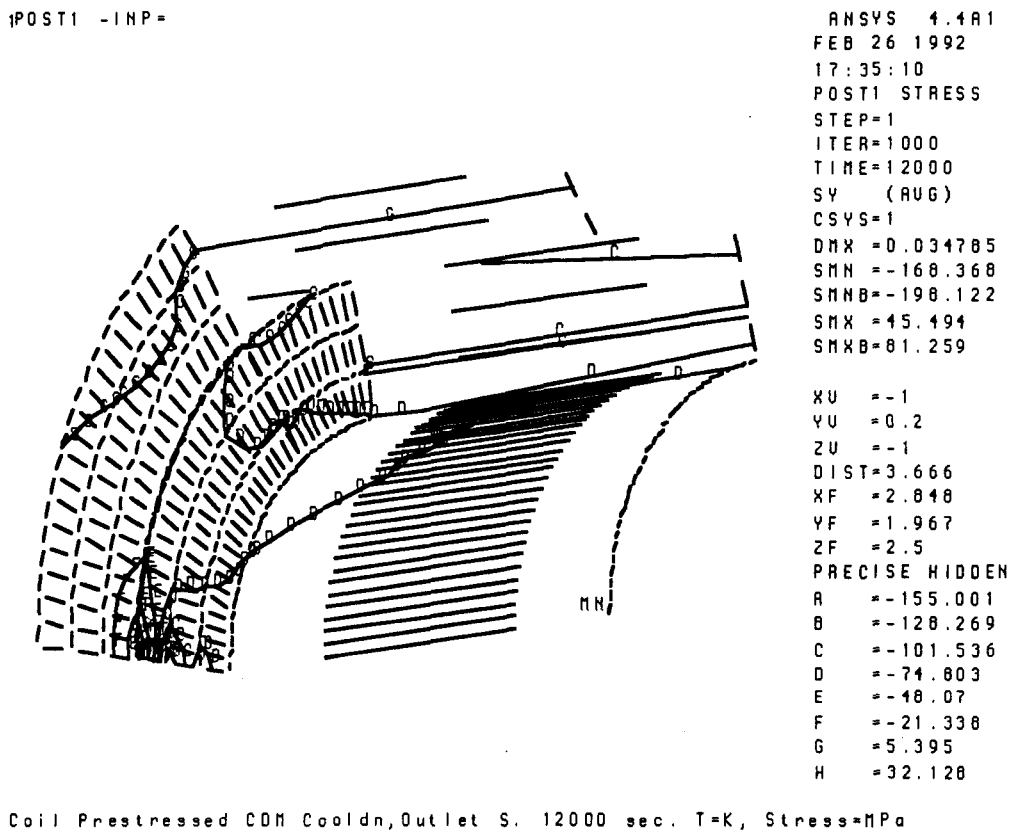

Figure 3. Figure 2 Thermal Transient Stress in Coils at 12,000 Seconds.

CONCLUSION

We have succeeded in understanding the major influence of the thermal transient effects on the CDM that are associated with differential thermal time constants of the yoke, shell, and end plate. Based on the assumption of using 4 K helium as the coolant to obtain

the fastest cooldown time at about 4 hours, we found that the cooldown local stress in the coil is about 23 ksi, and the maximum shell stress is about 184 ksi at the end shell where it joins the end plate. These stresses will certainly reduce by a factor of 2 or more, depending on the cooling process of the CDM. We also discovered that the end yoke is working very well to reduce the shell stress under thermal transient conditions. The shell is preloaded at room temperature, and the longitudinal welded joints of the shell are observed to reach yield-strength range. With additional cooldown thermal stress developed in the shell, the horizontal seam welds on the shell will reach beyond the allowable yield strength, producing the benefits of relaxing the residual stress in the shell and providing mechanical training of the magnet. The shell stress as calculated has not included the residual stress, preload, welded thermal, or external loadings in the shell.

Accelerated life tests need to be performed to identify potential fatigue-related failure modes at the skin welds. Also, a strain gauge assembly could be used to investigate the transient thermal stress build-up in the coil volume during cooldown.

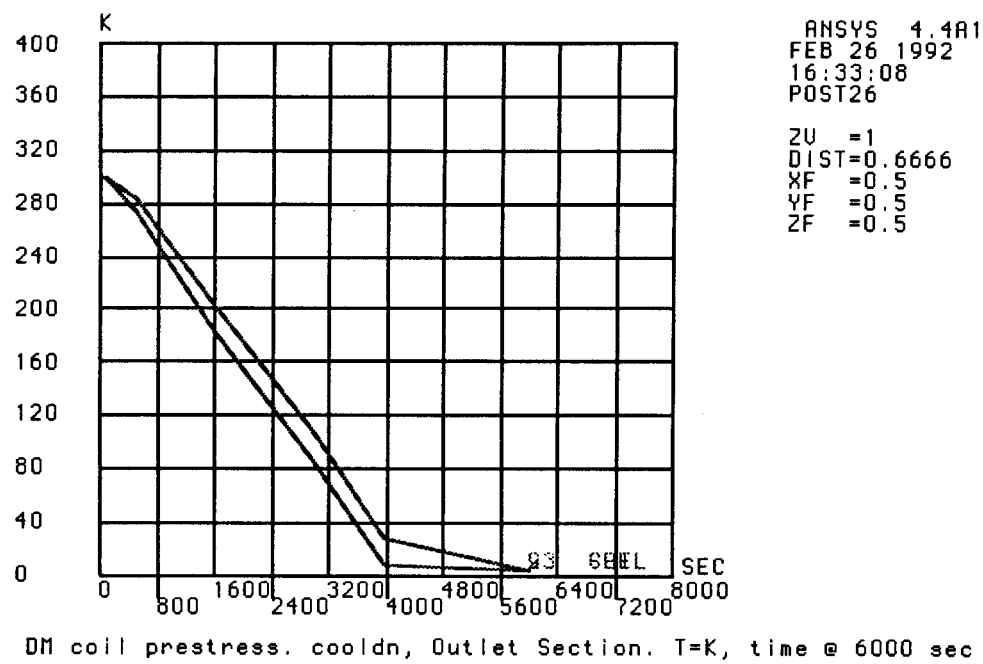

Note: Coil Temp.-Upper Curve. Shell Temp.-Lower Curve

Figure 4. Temperature-Time History of Coils at Center Section.

ACKNOWLEDGEMENT

The authors would like to acknowledge the contribution of B. Aksel of the SSC Laboratory.

REFERENCES

1. K. K. Leung, "An Engineering Design Study of the Dipole Magnet Cold Mass End Shell for the Superconducting Super Collider," page 287, *Supercollider 3*, edited by John Nonte, Plenum Press, New York, 1991.
2. B. Aksel and K. K. Leung, "Cooldown Stresses on the Coldmass of SSC Dipole Magnets," Conference Record 91CH3038-7, Vol. 4, pp. 2200–2202, *IEEE Particle Accelerator Conference,* 1991, San Francisco.
3. S. Delchamps, K.K. Leung, *et al.*, "SSC Collider Dipole Magnet End Mechanical Design," IEEE Particle Accelerator Conference Record 91CH3038-7, *Accelerator Science and Technology,* Volume 4, San Francisco, May 1991.
4. K. K. Leung, "Thermal Stress on Dipole Magnet Vessel End Shell," SSC Magnet System Division Report MD-TA-148, SSCL-N-702, April 1990.
5. J. Jayakumar, K. K. Leung, *et al.*, "Mechanical and Electromagnetical Analysis of 50 mm Designs for the SSC Dipole," *IEEE Transactions on Magnetics,* Vol. **27**, No. 2, March 1991.
6. K. K. Leung, "An Engineering Design Study of Detector Deformation Limits in the SSC SDC-Detector," Fourth Annual International Symposium on the Super Collider, March 1992.
7. T. Ogata *et al.*, "Low Cycle Fatigue and Other Mechanical Properties on Aged 316 Ln Stainless Steel at Liquid Helium Temperature," HY-05, ICMC 1989.